https://doi.org/10.5194/egusphere-2025-5904
Preprint. Discussion started: 4 December 2025

Microbial role in CO_2 fluxes along the river-estuary continuum in a rapidly uplifting catchment of eastern Taiwan

Jhen-Nien Chen[1], Pei-En Chen[2], Yu-Shiang Yen[1], Tzu-Hsuan Tu[3], Lu-Yu Wang[1], Wan-Yin Lien[1], Yueh-Ting Lin[2] and Pei-Ling Wang[2,4,5]

[1]Department of Geosciences, National Taiwan University, Taipei 106, Taiwan
[2]Institute of Oceanography, National Taiwan University, Taipei 106, Taiwan
[3]Department of Oceanography, National Sun Yet-sen University, Kaohsiung, Taiwan
[4]Research Center for Future Earth, National Taiwan University, Taipei 106, Taiwan
[5]Science and Technology Research Institute for Decarbonization, National Taiwan University, Taipei 106, Taiwan

Correspondence to: Pei-Ling Wang (plwang@ntu.edu.tw)

Abstract. The contribution of river metabolisms to carbon cycling is an essential issue, but not well examined in the catchment susceptible to the modulation of active tectonics. This study aims to quantify the rates of autotrophy and heterotrophy, and to identify the community compositions and potential members involved in these microbial processes in the Beinan River in eastern Taiwan. To address this, river water samples were collected in both the wet and dry seasons for incubations amended with ^{13}C-labeled dissolved carbon dioxide and amino acids. The analyses revealed a general pattern pointing to the higher rates in the wet season than in the dry season, and for heterotrophy than for autotrophy. The obtained rates were further scaled up, resulting in the catchment-scale CO_2 evasion of ~10^7 mole yr^{-1}, a range constituting several percent of the CO_2 flux derived from pyrite-induced weathering, oxidation of petrogenic carbon, and the river-air exchange. The community compositions generally varied with season for most upstream sites and with more abundant sulfur or nitrogen metabolizers in the wet season, as opposed to more abundant phototrophs or heterotrophs in the dry season. This study highlights the complex and dynamic nature of river metabolisms that contribute to carbon evasion in oligotrophic mountainous systems prone to the impacts of rapid uplift and erosion.

1. Introduction

Inland freshwater systems release CO_2 to the atmosphere at a flux (0.65-2.1 Pg-C yr^{-1}) comparable with that of ocean CO_2 uptake (2.2 Pg-C·yr^{-1}) (Horgby et al., 2019; Lauerwald et al., 2015; Takahashi et al., 2009). The magnitude is enormous given their limited area coverage of the global land surface (0.3-0.56%) (Allen and Pavelsky, 2018; Aufdenkampe et al., 2011). Among a variety of inland sub-systems, mountainous catchments, which comprise 27% of the Earth's land surface (Ives et al., 1997) and drain more than 30% of the global runoff, receive far less attention when compared with low-altitude catchments in temperate regions (Bandyopadhyay et al., 1997; Meybeck et al., 2001; Viviroli et al., 2004). While the accessibility to sampling or measuring in such high-relief catchments is often limited, a few previous studies have projected that CO_2 evasion declines substantially by orders of magnitude as a function of distance from the headwater (Raymond et al., 2013; Schelker et al., 2016; Chiriboga et al., 2023). Such a change of flux is intrinsically tied to the summed effect of P_{CO2} (CO_2 partial pressure) and exchange coefficient. Even fewer studies have further demonstrated that mountainous rivers draining the catchments composed of crystalline rocks are characterized by P_{CO2} slightly exceeding those in equilibrium with the atmospheric CO_2 (Horgby et al., 2019). Therefore, the enhanced CO_2 evasion in the upstream region could be largely attributed to the steep topography, where turbulent flow and rough river bed enable the rapid exchange of CO_2 between air and water. As the river slope decreases toward the downstream region, the degree of landscape-controlled CO_2 evasion diminishes gradually. The pattern highlights the role but also points out the deficiency in data coverage for mountainous catchments in configuring the global carbon inventory.

https://doi.org/10.5194/egusphere-2025-5904
Preprint. Discussion started: 4 December 2025

A number of factors have been considered to contribute to the overall pattern of CO_2 evasion along the river corridor. Among the factors involved in shaping its variation, groundwater input and *in situ* microbial processes are often considered the most important source mechanisms (Brunke et al., 1997; Cole et al., 2007; Marx et al., 2017). Measurements mostly using dissolved oxygen sensors have shown that aquatic metabolisms contributed to a sum of 28% of the CO_2 evasion for streams and rivers across the US continent (Butman and Raymond 2011; Hotchkiss et al., 2015). For mountainous catchments, most studies intuitively assume that groundwater input would dominate over *in situ* aquatic microbial processes in a way that the catchments are composed of exposed bedrocks rather than thick soils accumulated over a prolonged period of weathering and that the residence time of substrates is perhaps too short to be made available for microbial degradation (Marx et al., 2017; Duvert et al., 2018). Therefore, the quantities of the products derived from soil degradation (presumably attributed to dissolved organic carbon) would be scarce, thereby rendering the limited availability of substrates for microbial respiration. While the terrestrially derived fluxes (equivalent to lateral transport of groundwater) may dominate the CO_2 evasion in small streams and the aquatic metabolic fluxes may remain at a less variable level across stream orders, the percentage of aquatic metabolic flux to the overall evasion is postulated to increase with stream size (Hotchkiss et al., 2015). The exact fraction of metabolic flux to the overall evasion in mountainous rivers remains largely unconstrained.

The observations of diurnal variation in dissolved oxygen represent the net outcome combining primary production and ecosystem respiration. Therefore, the contribution of individual categories of metabolisms and further extrapolation to the CO_2 variation could only be deconvoluted with the computational scheme inherited with assumptions (Appling et al., 2018; Saccardi and Winnick, 2021). Furthermore, whether observations based on the cratonic continent or large river systems could be applicable to other catchments around the world remains less constrained. In particular, small island catchments susceptible to active tectonics are constantly impacted by torrential precipitation associated with monsoons and cyclones, mass wasting processes, and structurally controlled transport of groundwater (McMillan et al., 2015). The event-based hydrological and geological impacts would have led to a pattern of nutrient and substrate availability (e.g., turbid river water during high water) and transport of microbial populations fundamentally distinct from the major river systems. Furthermore, while benthic and hyporheic processes dominate overall metabolic fluxes in some systems, turbid, high-energy rivers with limited light penetration and frequent sediment mobility present challenging conditions that constrain both benthic and planktonic metabolism (Battin et al. 2023; Hall et al., 2015). In mountainous catchments with steep gradients, frequent sediment transport, and chronically turbid water, planktonic processes may constitute the primary measurable component of aquatic metabolism. Dissecting the fractions of individual metabolisms to the net ecosystem respiration rates for planktonic metabolisms would pave the way to unveil the complex carbon cycling and metabolic network along the river corridor.

In this study, we aimed to quantify planktonic metabolic rates and characterize microbial community dynamics along the Beinan River, a system where the sediment exports and weathering rates rank among the greatest in Taiwan (Dadson et al., 2003). Instead of measuring dissolved oxygen variations to infer bulk/net respiration rates, short-term incubations supplemented with ^{13}C-labeled dissolved inorganic carbon (DIC) and amino acids (leucine and glycine) were adopted to constrain assimilation and respiration rates of different metabolisms. The approach of directly measuring CO_2 assimilation and production overcomes the limitation that the net ecosystem production rate could not be appropriately recovered due to the lack of oxygen variation for the turbid water commonly encountered during high water season. Since the supplemented amino acids are essential for heterotrophy, the derived rates also enable the determination of the efficiency of anabolism versus catabolism. The summed rates were compared with the rates of CO_2 produced from weathering reactions, constrained by solute abundances and isotopic compositions, and with the rates of gas exchange between river

https://doi.org/10.5194/egusphere-2025-5904
Preprint. Discussion started: 4 December 2025

water and the atmosphere to draw the inference of the effect of aquatic metabolisms on river carbon dynamics. Finally, microbial community compositions were characterized based on 16S rRNA gene tags prior to the incubations to identify potential metabolic groups associated with measured activities.

2. Materials and methods

2.1 Field background

Taiwan was formed through dual subduction and interactions between the Eurasian and Philippine Sea Plates (Teng 1990). The northwestward impingement of the Luzon arc on the Eurasian continent since 5 Ma has created steep topographic changes with the unroofing of metamorphic complexes in the backbone range, from which major rivers originate (Chen et al., 2019). Across the island (particularly central and southern Taiwan), rapid uplift (up to several centimeters per year), river incision, event-based torrential precipitation, and frequent earthquakes have generated numerous landslides with sediments transported along with flow or temporarily deposited in the riverbank/bed and subsequently remobilized during the high water period (Dadson et al., 2003; Kao and Milliman, 2008). The Beinan River, which is one of the largest rivers in Taiwan in terms of discharge and suspended sediment load (Dadson et al., 2003; Kao and Milliman, 2008; annual report of the Water Resource Agency, MOEA), flows eastward across the central mountain and drains southward along the Longitudinal Valley prior to reaching the ocean. The catchment covers an area of ~1600 km^2 and is primarily composed of schist and slate, with minor amounts of marble and meta-sandstone (Stanley et al., 1981). The soil development is limited and hindered by high erosion rates. Therefore, detritus materials that are susceptible to pulverization and abrasion are primarily composed of rock fragments. Previous studies based on carbon isotopic compositions and radiocarbon contents have inferred a negligible contribution of soil to particulate organic matter (Hilton 2008; Lin et al., 2020). Monsoon combined with typhoon from summer to autumn contributes the majority of precipitation (generally >3000 mm) and runoff in the upstream region. For this study, the wet season was referred to the period between May and November 2020 during which the precipitation accumulated substantially (Fig. S1). Notably, May is referred to as the dry season considering that the field campaign in May of 2020 was conducted prior to the significant increase in precipitation in late May (Fig. S1). It is also worth noting that the sampling period represents the driest year (annual precipitation of 1856 mm) over the last 20 years.

2.2 Sampling and field experiments

Water samples were collected and characterized at five sites ranging from upstream to downstream (MLL01, CWL01, DL, LY04, and BNE; Figs. 1 and S1) along the Beinan River and its tributaries between January 2020 and January 2021. A total of seven field campaigns were conducted in January, March, May, July, August, and October 2020 and January 2021 (Table S1). While *in situ* environmental parameters were characterized in all campaigns, metabolic rates were measured in March and May 2020 (for phototrophy and autotrophy only) and in August 2020 and January 2021 (for the full suite of tested metabolisms). At each site, *in situ* physicochemical characteristics (temperature, pH, conductivity, and river flow rate) were measured using the portable probes and meters (Hanna Instruments, HI-98130, RI, USA; Pro II SVR, Stalker, TX, USA). Samples were collected in different forms with different preservatives and preparations (Wang et al., 2024). In brief, river water was filtered using sterilized 0.22 μm pore-size cellulose membranes and collected for analyses of dissolved inorganic carbon (DIC), major cations and anions, dissolved organic carbon (DOC), and nutrients (nitrate, nitrite, ammonium, and orthophosphate). Syringes and bottles for DOC and cation samples were pre-washed with concentrated nitric acid and the filtered river water to remove potential contaminants absorbed on the apparatus. Cation samples were acidified with 1/10 volume of 20% nitric acid (Baseline grade, Seastar, BC, Canada). Samples were stored at room temperature (for DIC and inorganic solutes) or –20 °C (for DOC and nutrients). Particulate samples were collected

https://doi.org/10.5194/egusphere-2025-5904
Preprint. Discussion started: 4 December 2025

on 0.3 μm pore-size glass fiber membranes pre-combusted at 500 ºC for 6 hours to remove any potential organic contaminants. Carbonate minerals captured by membranes were removed with 2 N HCl immediately after the filtration. The total volume of filtrate for individual particulate samples was 1 L. The membranes were frozen at either –20 ˚C for analyses of chlorophyll a (chl-a) and abundances and isotopic compositions of particulate organic carbon (POC), or –80 ˚C for molecular analyses.

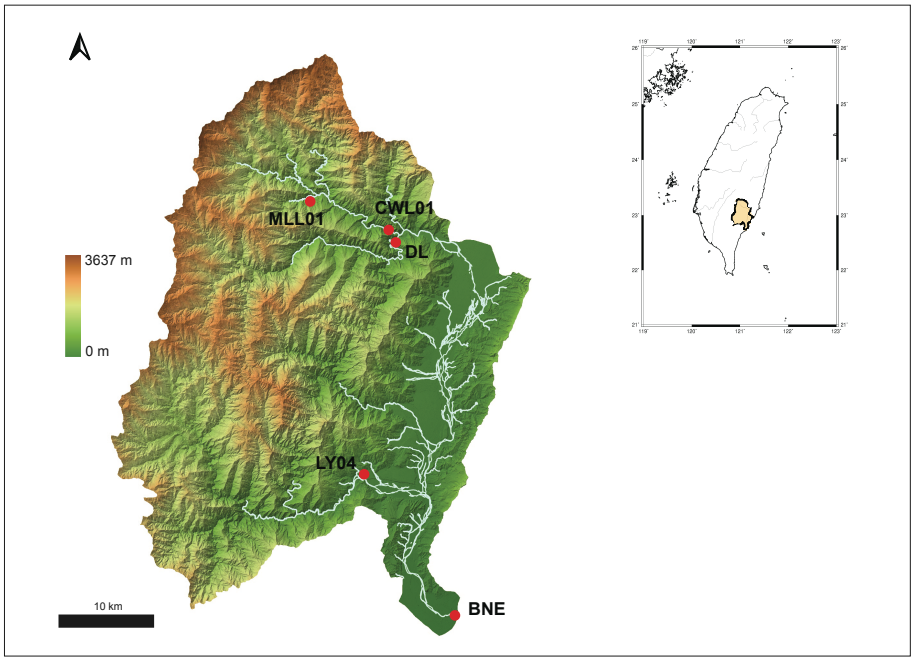

Figure 1: Topographic map of Beinan River system and sampling sites marked by red points.

For metabolic rate measurements, river water was collected into a water bag pre-washed with river water several times, and supplemented with ^{13}C-labeled bicarbonate or individual amino acids ([1-^{13}C]glycine or [1-^{13}C]L-leucine at a final concentration of 50 μM to constrain the rates of autotrophy/phototrophy (using DIC) and heterotrophy/respiration (using amino acids). The supplemented substrates with a ^{13}C purity of >99% were mixed with deionized water to generate a stock at a concentration of 1 mM. The stock for amino acids was acidified by titrating with HCl to pH <4 so the potential DIC associated with the dissolution of the amino acid powder could be removed. The stock of either DIC or amino acid was filter-sterilized and stored at 4 ˚C until further use in the field. The chosen concentration was either much lower than the environmental DIC concentrations (1-2 mM; Wang et al., 2024) or comparable with the environmental DOC concentrations (20-80 μM). In this context, the measured autotrophic and phototrophic rates are considered to be representative of *in situ* rates, whereas the measured organic assimilation and respiration rates might be stimulated due to the slightly enhanced supply of substrates. The supplemented river water was then dispensed into transparent or opaque polycarbonate bottles and incubated under constant illumination (~18000 lux, monitored by HOBO, Pandant MX) for 4 to 6 hours at room temperature maintained by running water. The incubated samples were filtered using 0.3 μm pore-size glass fiber membranes to collect particulates that represent a sum of mineral/rock fragments and microorganisms. The membranes were rinsed with 2 N HCl immediately after the filtration to remove carbonate minerals and then washed with

https://doi.org/10.5194/egusphere-2025-5904
Preprint. Discussion started: 4 December 2025

sterilized saline solution. The collected membranes were stored at –80 ºC for further isotopic and molecular analyses. Part of the filtrates for the incubations with amino acids were preserved and stored at room temperature for isotopic analyses of DIC. A conceptual diagram describing the experimental setup is shown in Fig. 2.

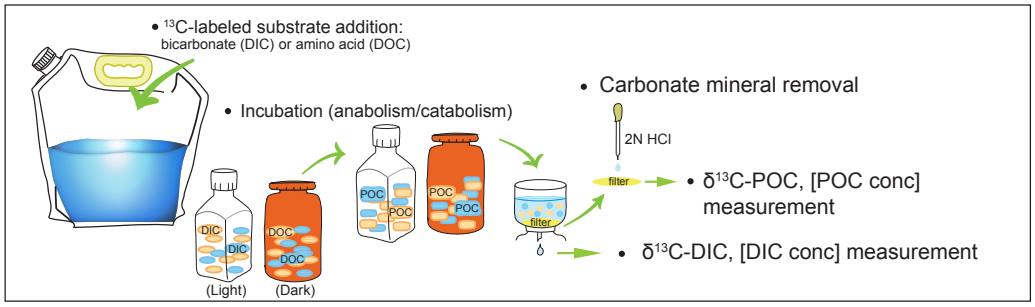

Figure 2: Conceptual diagram for the incubation setup in fields and following laboratory measurments.

2.3 Geochemical analyses

Anions were measured using an ICS-3000 ion chromatography (Thermo Fisher Scientific, USA). Major cations were analyzed using an inductively coupled plasma linked with a quadrupole mass spectrometry (ICPMS; 7800, Agilent Taiwan, Taiwan). Synthetic and river water standards (SLRS-5 from the National Research Council of Canada) were used to calibrate a range of cation concentrations. Concentrations of orthophosphate and ammonium were measured on molybdenum blue generated from the reductive reaction between phosphate complex and ascorbic acids (APHA Method 4500-P, 2005), and indophenol generated from the reaction between ammonium and thymol (APHA Method 4500-NH3, 2005), respectively. The intensity of the color complex was quantified using a spectrophotometer (V-500, Jasco, MD, USA). Nitrite/nitrate concentrations were quantified using a commercial fluorometric assay (Cayman, MI, USA), which reacts nitrite (*in situ* or reduced from nitrate) with 2,3-diaminonaphthalene for the generation of 1(H)-naphthotriazole (Miles et al., 1995). Chlorophyll a was extracted from membranes with acetone under dark conditions and quantified using a fluorometer (10-AU, Turner Designs, CA, USA). The analytical uncertainty for these methods is less than 2%. DOC concentration was measured using a Shimadzu TOC-L CPH/CPN system with high-temperature catalytic oxidation, employing KHP (potassium hydrogen phthalate) as the standard. Concentrations and carbon isotopic compositions of DIC were analyzed by acidifying samples with concentrated phosphoric acid (85%) and purging the produced CO_2 into a total carbon analyzer (Aurora 1030, OI Analytical, USA) and an isotope ratio mass spectrometer (IRMS; MAT253, Thermo Fisher Scientific, USA)) connected with a GC-IsoLink (Thermo Fisher Scientific, USA), respectively. Concentrations and carbon isotopic compositions of particulate organic carbon (POC) were analyzed on freeze-dried, acid-rinsed membranes using an elemental analyzer (EA; MICRO cube, Elementar, Germany) and an IRMS (Delta V) coupled to a Flash EA (Thermo Fisher Scientific, USA), respectively. Carbon isotopic compositions were expressed as the delta notation:

$$\delta^{13}C = \left[\frac{R_{sample}}{R_{standard}} - 1\right] \times 1000\ ‰ \quad (1)$$

where R is the ratio of ^{13}C to ^{12}C, and the standard is Vienna Pee Dee Belemnite (VPDB). The uncertainties for DIC and POC concentrations and $\delta^{13}C$ values were less than 2% and 0.2 ‰, respectively. Metabolic rates were calculated using the following equations:

https://doi.org/10.5194/egusphere-2025-5904
Preprint. Discussion started: 4 December 2025

$$R_{DIC-uptake} = \frac{\Delta F^{13}C_{POC}}{F^{13}C_{DIC}} \times [POC] \times \frac{1}{t} \quad (2)$$

$$R_{AA-total} = R_{AA-uptake} + R_{AA-catabolic} = \frac{\Delta F^{13}C_{POC} \times [POC] + \Delta F^{13}C_{DIC} \times [DIC]}{F^{13}C_{DOC}} \times \frac{1}{t} \quad (3)$$

where R represents the metabolic rate of either DIC assimilated into biomass ($R_{DIC\text{-}uptake}$) or specific amino acid assimilated into biomass plus oxidized into DIC ($R_{AA\text{-}total}$), $F^{13}C$ represents the fraction of ^{13}C in POC, DIC, or DOC, [POC] and [DIC] are the measured POC and DIC concentrations, respectively, and t is the duration of incubation. The isotopic fractionation associated with the target metabolic reaction is assumed to be negligible. In this regard, the $F^{13}C_{DIC}$ in eq. 2 and $F^{13}C_{DOC}$ in eq. 3 was the sum of the ^{13}C fractions of added substrate and original forms (DIC or DOC). The $\delta^{13}C$ values of *in situ* DOC were not available and, therefore, assumed to be –27 ‰ considering the isotopic compositions of soil organic matter were in a similar range (Wang et al., 2024; Lien et al., 2025). The rate for the incubation with DIC under light is often considered to represent the summed rate of phototrophy and lithoautotrophy, and could be greater than the rate for the dark incubation. The difference is generally attributed to the phototrophic rate, assuming the true lithoautotrophy is not affected by light illumination.

2.4 Molecular analyses of community compositions

Crude DNA was extracted and purified using the DNeasy PowerSoil kit (Qiagen, USA) following the manufacturer's protocol, and stored at –80 ˚C for further analyses. Polymerase chain reaction (PCR) amplification was conducted on all extracts using the primers 515F (GTG CCA GCM GCC GCG GTA A) and 806R (CCC GTC AAT TCM TTT RAG T), which target the V4 region of the 16S rRNA gene (Kozich et al., 2013). The amplicons were purified, pooled, barcoded, and sequenced using the Illumina MiSeq platform (Illumina, USA). The detailed methodology and reagents employed for PCR have been described in Tu et al., (2017, 2022). Due to the insufficient quantity of DNA (<50 ng in total), extracts for incubated samples were not further processed for stable isotope probing, which targets the population members actively assimilating the fed ^{13}C-labeled substrate.

Quantitative PCR (qPCR) was performed to determine the copy numbers of bacterial and archaeal 16S rRNA genes and genes encoding ribulose-1,5-bisphosphate carboxylase/oxygenase forms I (*cbb*L) (Alfreider et al., 2003) using the QuantStudio ™ 3 Real-Time PCR System (Applied Biosystems, ABI, USA). The standard preparations and PCR conditions were as described in Tu et al., (2017) and Wang et al., (2014). The primers and annealing temperatures for the different genes are summarized in Table 1. The copy number was calculated using the threshold cycles calibrated against standards with known concentrations of gene amplicons, assuming 650 g mol^{-1} for DNA molecules.

Raw sequences of 16S rRNA gene amplicons were processed using Mothur ver. 1.48.0 (Schloss et al., 2009) and QIIME2 (Bolyen et al., 2019). The individual reads were quality-filtered, denoised, merged, and dechimerized to generate Amplicon Sequence Variants (ASVs). Taxonomic classification was performed using the SILVA database (version 138) (Quast et al., 2012). Sequence reads were rarefied through 100 sequence random re-sampling (without replacement) to account for the difference in sequencing depth for the calculation of alpha diversity indices, such as observed ASVs and Chao1 for richness (Chao et al., 1987), and Shannon index for evenness (Shannon and Weaver 1949). For beta diversity, the entire ASV table was used and normalized. Correlations between microbial communities and environmental factors were determined using canonical correspondence analysis (CCA) (González et al., 2008). All statistical analyses were performed using R with the vegan, ggplot2, and phyloseq packages. The obtained sequences were deposited in GenBank (BioProject ID: PRJNA1270665).

Table 1: Primer information in this study.

Primer name	Sequence (5'-3')	Target group/gene	Annealing temp (°C)	Reference
B27F	AGAGTTTGATCMTGGCTCAG	Bacteria/16S rRNA	55	Lane (1991)
Eub338R	GCTGCCTCCCGTAGGAGT	Bacteria/16S rRNA	55	Amann et al. (1990)
U1492R	GGTTACCTTGTTACGACTT	Bacteria/16S rRNA	55	Lane (1991)
A8F	TCYGGTTGATCCTGCC	Archaea/16S rRNA	55	Huber et al. (2002)
A806F	ATTAGATACCCSBGTAGTCC	Archaea/16S rRNA	55	Takai and Horikoshi (2000)
A958R	YCCGGCGTTGAMTCCAATT	Archaea/16S rRNA	55	Hinrichs et al. (1999)
U1513R	ACGGHTACCTTGTTACGACTT	Archaea/16S rRNA	55	Huber et al. (2002)
cbbLR1F	AAGGAYGCGAGAACATC	autotroph/*cbb*L	58	Selesi et al. (2007)
cbbLR1intR	TGCAGSATCATGTCRTT	autotroph/*cbb*L	58	Selesi et al. (2007)

https://doi.org/10.5194/egusphere-2025-5904
Preprint. Discussion started: 4 December 2025

2.5 Computation for catchment scale CO_2 fluxes

To scale planktonic metabolic rates to the catchment level, measured rates were multiplied by the average water depth of each investigated reach (50 cm for tributaries, 70 cm for main stem) to obtain areal fluxes. These depth estimates reflect typical conditions observed during field campaigns, excluding flash flood periods. DIC uptake rates under light and dark conditions were assumed to represent daytime and nighttime rates, respectively, with total daily DIC uptake calculated as the sum of equal contributions from each. Using leucine incorporation rates as a conservative estimate of heterotrophic activity, net CO_2 production for each sub-catchment and summed across the catchment was calculated assuming river surface area represents 0.47% of the total catchment area (1584 km²; Raymond et al., 2013).

To compare the metabolic fluxes with the CO_2 evasion, CO_2 exchange fluxes between river water and atmosphere were calculated for each sub-catchments using the following equation:

$$\text{Flux} = k_{CO2} \times \text{delta}\ (C_{measured} - C_{eq}) \quad (4)$$

where k_{CO2} is the gas exchange velocity, and C represents the partial pressure of CO_2 either from measurement or in equilibrium with the atmospheric CO_2 concentration (assumed to be 410 ppm). $C_{measured}$ was derived from the DIC concentration, pH, salinity, temperature, and total atmospheric pressure measured in the same field campaign using co2sys (Lewis and Wallace, 1998). k_{CO2} was computed using the relationships reported by Ulesth et al. (2019), where k_{600} values vary positively with eD (energy dissipation rate and is equal to the product of g (gravitational acceleration), v (flow velocity) and s (slope of the reach)). Depending on whether the gas exchange is controlled by turbulence or bubble, the relationships between k_{600} and eD are different (Ulseth et al., 2019):

$$\text{Ln}\ k_{600} = 6.43 + 1.18 * \text{Ln eD (for eD} > 0.02) \quad (5)$$

$$\text{Ln}\ k_{600} = 3.10 + 0.35 * \text{Ln eD (for eD} < 0.02) \quad (6)$$

The flow velocity was adopted from the measured ones obtained from the field, which represented the maximum velocity on the river surface. Because friction would be substantial near the channel bed, the measured surface velocity would be higher than the average channel velocity integrated over the channel cross section. However, considering the water depth is generally small, the measured flow velocity may not substantially deviate from the true one. Nevertheless, the calculated eD values would represent an overestimate. Slope was calculated for the investigated reach (~1000 m in length) using the DEM (digital elevation model) available for the public (data.gov.tw). All the parameters used for calculation were summarized in Table S6. The obtained k_{600} value was further converted to k_{CO2} using the following equation (Wanninkhof, 2014):

$$k_{CO2} = k_{600} / [(600 / Sc_{CO2})]^{(-n)} \quad (7)$$

where Sc is Schmidt number of CO_2 at the in situ temperature and n is assumed to be 0.5 for turbulent water (Jähne et al., 1987).

3. Results

Physicochemical characteristics for each field campaign were categorized into the wet and dry seasons in accordance with the precipitation records (Tables 2, S1; Fig. S1). Among all the environmental parameters, several were significantly different between the wet and dry seasons, including water temperature, TSM, POC, carbon isotopic compositions of POC ($\delta^{13}C_{POC}$), DOC, and NH_4^+ (Wilcoxon test, $p < 0.05$) (Tables 2, S1). Water temperatures varied between 12 and 30 °C and were highly dependent on the altitude. TSM contents ranged between several to hundreds of mg L^{-1}. POC

https://doi.org/10.5194/egusphere-2025-5904
Preprint. Discussion started: 4 December 2025

concentrations were higher in the wet season than in the dry season with a factor of up to 50 (for LY04). The $\delta^{13}C_{POC}$ values ranged between –28 and –20 ‰, and tended to be smaller (more negative) in the dry season (varied by different degrees between sites). Ammonium concentrations ranged between 0.3 and 16.5 µM and were higher in the wet season than in the dry season. For comparison, concentrations of other nutrients (nitrate/nitrite and phosphate) and Chl-a varied to different degrees. For any individual sites, nitrate/nitrite and phosphate concentrations ranged between 1.7 to 48.3 µM and between 0.01 and 0.31 µM, respectively, and were indistinguishable between seasons (Wilcoxon test, $p > 0.05$). Chl-a concentrations ranged from lower than the detection limit to 2.1 mg m^{-3} and were generally higher in the dry season than in the wet season (except for DL). DIC concentrations and their $\delta^{13}C$ values varied between 1.26 and 2.88 mM and between –6.8 and +0.6 ‰, respectively. The variation was generally indistinguishable between sites and seasons (t-test, $p > 0.05$). The exception occurred for the estuarine site (BNE), where DIC was most depleted in ^{13}C. Sulfate concentrations ranged between 1.03 and 2.06 mM for most sites with the exception of MLL01 (2.92–3.59 mM).

Table 2: Physicochemical characteristics among sites and seasons.

		T[1] (°C)	pH	**TSM**[1] (mg/L)	**POC** (mg m^{-3})	**δ^{13}C-POC** (‰)	**DOC** (μM)	DIC (mM)	δ^{13}C-DIC (‰)	Chl a (mg m^{-3})	TIN[2] (μM)	NH_4^+ (μM)	PO_4^{2-} (μM)	SO_4^{2-} (mM)
Tributary (altitude)	n (sample numb. for wet or dry season)	n= 4, 3	n= 4, 3	n= 2, 3	n= 2, 3	n= 2, 3	n= 4, 3	n= 3, 3	n= 4, 3	n= 3, 2	n= 4, 3	n= 3, 3	n= 4, 3	n= 3, 3
MLL01 (699 m)	Wet seasons	23.4 ± 2.8	8.4 ± 0.4	157 ± 113	2432 ± 1868	-24.3 ± 0.3	30.4 ± 12.96	1.92 ± 0.05	-1.8 ± 2.1	0.07 ± 0.06	10.0 ± 2.5	4.6 ± 4.3	0.04 ± 0.05	3.36 ± 0.21
	Dry seasons	17.3 ± 4.7	8.1 ± 0.5	11 ± 16	152 ± 32	-27.4 ± 0.3	20.63 ± 1.71	1.91 ± 0.34	-2.7 ± 1.3	0.44 ± 0.08	6.8 ± 6.2	0.6 ± 0.3	0.05 ± 0.04	3.02 ± 0.13
	Total	20.8 ± 4.7	8.2 ± 0.4	70 ± 98	1064 ± 1560	-26.1 ± 1.7	26.21 ± 10.59	1.92 ± 0.21	-2.2 ± 1.8	0.22 ± 0.21	8.7 ± 4.3	2.6 ± 3.5	0.05 ± 0.04	3.19 ± 0.24
CWL01 (375 m)	Wet seasons	26.1 ± 2.4	7.8 ± 0.1	27 ± 32	1477 ± 1381	-23.4 ± 2.7	31.22 ± 16.03	1.81 ± 0.48	-2.8 ± 1.3	0.58 ± 0.38	6.0 ± 0.8	4.9 ± 1.9	0.06 ± 0.04	1.53 ± 0.04
	Dry seasons	20.2 ± 6.8	8.5 ± 0.3	12 ± 18	236 ± 129	-26.8 ± 1.0	23.96 ± 3.30	2.18 ± 0.37	-2.1 ± 1.9	1.33 ± 1.02	5.2 ± 3.9	2.5 ± 0.6	0.04 ± 0.03	1.61 ± 0.04
	Total	23.1 ± 5.6	8.2 ± 0.4	18 ± 22	732 ± 973	-25.4 ± 2.4	28.11 ± 12.13	1.99 ± 0.43	-2.5 ± 1.5	0.83 ± 0.67	5.7 ± 2.3	3.7 ± 1.8	0.05 ± 0.03	1.57 ± 0.06
DL (382 m)	Wet seasons	26.6 ± 2.2	7.9 ± 0.6	4 ± 3	291 ± 24	-25.9 ± 0.2	35.39 ± 19.96	2.16 ± 0.05	-1.9 ± 0.9	1.14 ± 0.54	16.0 ± 4.2	6.4 ± 6.5	0.14 ± 0.02	1.08 ± 0.04
	Dry seasons	21.9 ± 7.3	8.4 ± 0.2	11 ± 18	160 ± 63	-26.4 ± 0.4	20.26 ± 3.40	2.43 ± 0.41	-1.9 ± 0.6	0.64 ± 0.24	18.0 ± 3.0	1.5 ± 1.3	0.15 ± 0.06	1.13 ± 0.12
	Total	24.6 ± 5.2	8.2 ± 0.5	8 ± 13	212 ± 86	-26.2 ± 0.4	28.9 ± 16.38	2.29 ± 0.30	-1.9 ± 0.7	0.94 ± 0.48	16.8 ± 3.6	4.3 ± 5.4	0.14 ± 0.04	1.11 ± 0.08
LY04 (238 m)	Wet seasons	27.4 ± 2.3	8.0 ± 0.2	499 ± 172	9361 ± 4358	-20.4 ± 0.3	22.97 ± 4.02	2.30 ± 0.38	-2.9 ± 1.4	0.05 ± 0.09	9.6 ± 4.5	7.1 ± 3.2	0.08 ± 0.03	1.70 ± 0.24
	Dry seasons	21.1 ± 6.0	8.4 ± 0.3	15 ± 15	174 ± 48	-27.5 ± 0.4	17.42 ± 3.94	2.34 ± 0.43	-3.9 ± 1.0	0.37 ± 0.09	8.3 ± 2.8	2.2 ± 0.7	0.07 ± 0.00	1.41 ± 0.06
	Total	24.7 ± 5.1	8.2 ± 0.3	208 ± 280	3849 ± 5484	-24.7 ± 3.9	20.59 ± 4.7	2.41 ± 0.32	-3.3 ± 1.2	0.18 ± 0.19	9.0 ± 3.6	4.7 ± 3.4	0.07 ± 0.02	1.56 ± 0.22
BNE (7 m)	Wet seasons	28.0 ± 2.6	7.8 ± 0.1	106 ± 131	2282 ± 2718	-25.0 ± 1.4	45.13 ± 22.48	2.58 ± 0.45	-4.9 ± 2.5	0.78 ± 1.03	31.0 ± 14.1	7.3 ± 6.2	0.19 ± 0.09	1.84 ± 0.20
	Dry seasons	21.5 ± 6.8	8.4 ± 0.3	12 ± 17	245 ± 73	-26.4 ± 0.6	35.62 ± 10.05	2.02 ± 0.28	-5.7 ± 0.2	1.73 ± 0.43	30.1 ± 10.5	1.7 ± 0.2	0.25 ± 0.07	1.46 ± 0.09
	Total	25.2 ± 5.5	8.4 ± 0.2	49 ± 84	1060 ± 1759	-25.8 ± 1.1	41.05 ± 17.67	2.30 ± 0.45	-5.2 ± 1.8	1.16 ± 0.92	30.6 ± 11.7	4.9 ± 5.3	0.21 ± 0.08	1.65 ± 0.25

* Parameters shown in bold are significantly different between two seasons (Wilcoxon test, $p < 0.05$). Detailed data are provided in Table S1.
[1] T: water temperature; TSM: total suspended matter.
[2] TIN includes nitrate and nitrite (nitrite was below detection limit).

https://doi.org/10.5194/egusphere-2025-5904
Preprint. Discussion started: 4 December 2025

Uptake rates for ^{13}C-labeled DIC under light conditions varied from 0.04 to 1.98 mgC m^{-3} hr^{-1} (Fig. 3a; Table S2). The rates measured in August were either higher than (for MLL01, LY04, and BNE) or comparable (for CWL01 and DL) with those in other months. The rates were also higher at sites near the estuary (BNE) than at other upstream sites by a factor of at least 2. In contrast, incubations with ^{13}C-labeled DIC under dark conditions exhibited a drastically different pattern (Fig. 3b). Most rates were either below the detection limit or less than 0.05 mg C m^{-3} hr^{-1}. Exceptions occurred for sites MLL01 (0.7 mgC m^{-3} hr^{-1}), LY04 (1.6 mgC m^{-3} hr^{-1}), and BNE (0.19 mgC m^{-3} hr^{-1}) in August.

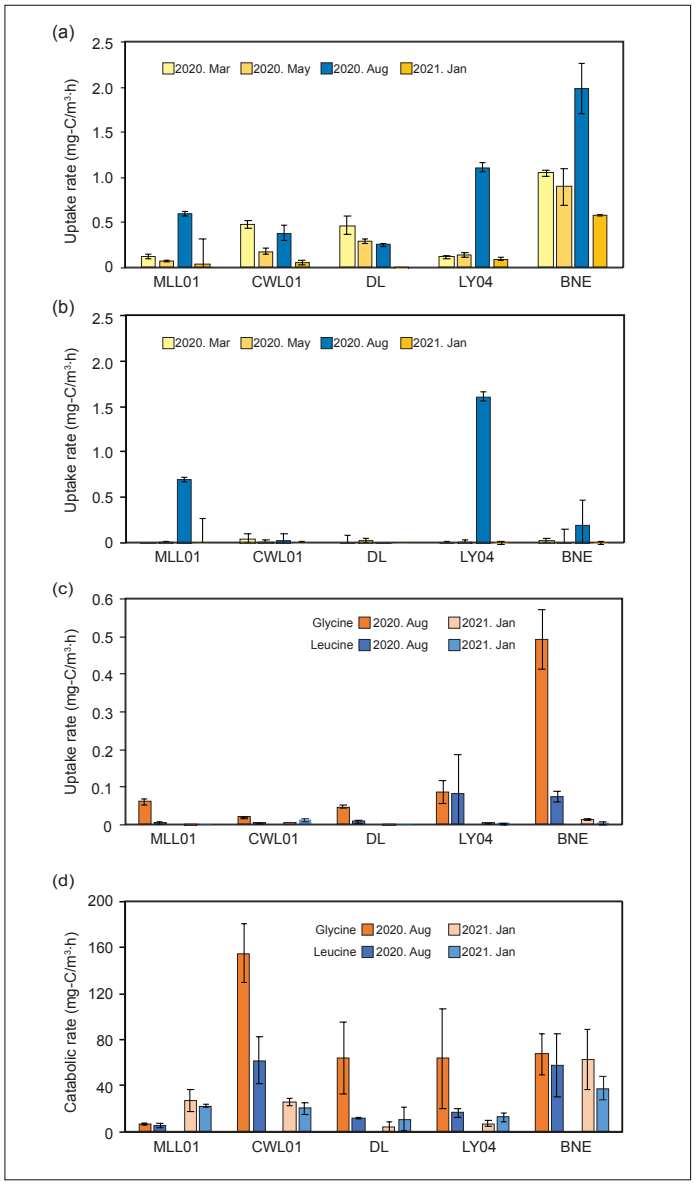

Figure 3: Carbon transformation rates of autotrophy and heterotroph. Uptake rates of DIC under light (A) and dark (B) conditions. Uptake rates (C) and catabolic rates (D) of amino acids.

https://doi.org/10.5194/egusphere-2025-5904
Preprint. Discussion started: 4 December 2025

Uptake rates of incubations with ^{13}C-labeled amino acids ranged from lower than the detection limit to 0.49 mgC m^{-3} hr^{-1} (Fig. 3c; Table S2). These rates were generally higher in August than in January regardless of sites. Uptake rates with glycine were higher than those with leucine except for LY04 in August. For comparison, catabolic rates ranged from 4.5 to 154.4 mg C m^{-3} hr^{-1} and varied spatially and temporally (Fig. 3d; Table S2). Catabolic rates with glycine were also higher than those with leucine in most incubations regardless of sites and time (except for DL and LY04 in January). While they were higher in August than in January at sites CWL01, DL, and LY04, they were comparable between the two months at site BNE. By contrast, the catabolic rates at MLL01 were higher in January than in August. Most of the added amino acids were utilized for respiration (as the product of total CO_2; >99%) rather than biosynthesis.

Scaling measured rates to the catchment level yielded net metabolic CO_2 production fluxes of 5.16 mol m^{-2} yr^{-1} for MLL01, 21.11 mol m^{-2} yr^{-1} for CWL01, 4.22 mol m^{-2} yr^{-1} for DL, 5.35 mol m^{-2} yr^{-1} for LY04, and 24.44 mol m^{-2} yr^{-1} for BNE (Supporting Information Table S5). The total yield of planktonic metabolic CO_2 for individual sites ranged from 10^5 to 10^7 mol yr^{-1}, with a catchment-wide total of ~10^7 mol yr^{-1}. For comparison, areal CO_2 evasion fluxes ranged from 0.20–1.76 mol m^{-2} d^{-1} for CWL01, 3.97–17.3 mol m^{-2} d^{-1} for MLL01, 0.27–0.73 mol m^{-2} d^{-1} for DL, 0.39–1.56 mol m^{-2} d^{-1} for LY04, and 0.20–0.90 mol m^{-2} d^{-1} for BNE (Supporting Information Table S6). Summing exchange rates across the catchment yielded a total annual emission of approximately 2.6×10^9 mol yr^{-1}.

Bacterial and archaeal 16S rRNA gene abundances for river water ranged from 2.3×10^3 to 3.9×10^7 copies·L^{-1} and from 5.6×10^4 to 5.5×10^6 copies·L^{-1}, respectively (Fig. S2). The abundances of *cbb*L ranged from 1.8×10^3 to 7.2×10^5 copies L^{-1}. The gene abundances were generally higher in January than those in other months (mostly by more than one order of magnitude) except at BNE. The difference between gene abundances in January and August was even more pronounced for LY04. By comparison, the gene abundances for BNE were less variable between seasons (or months) when compared with those at the other sites.

A total of 532,787 reads of 16S rRNA gene amplicons were obtained and classified into 13,005 ASVs. The observed ASVs and Chao1 based on the rarefied dataset (n=5220) ranged between 200 and 1600 and between 150 and 2300, respectively (Table S3). For comparison, the Shannon index spanned from 4.4 to 6.9. The variations of these indices were generally comparable to each other and showed different patterns among sites and sampling intervals (Fig. 4a). In particular, indices for sites MLL01 and LY04 were lower in the wet season than in the dry season (except for January sample for MLL01). For the other three sites (CWL01, DL, and BNE), these indices were generally less variable through time. However, indices for January samples of CWL01 and BNE and the July sample of BNE deviated substantially from those for the rest of the samples.

https://doi.org/10.5194/egusphere-2025-5904
Preprint. Discussion started: 4 December 2025

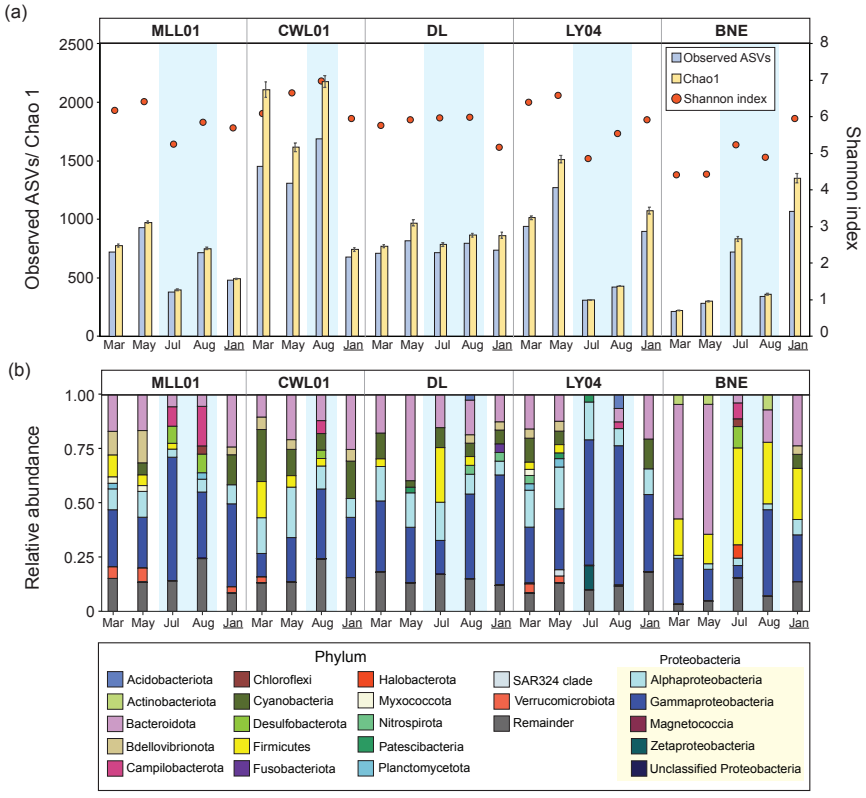

Figure 4: (A) Alpha diversity indices and (B) community compositions based on 16S rRNA genes for river samples. Time intervals with blue background represent the wet season.

Community compositions varied temporally and spatially to different degrees with the major phyla including Bacteroidota, Cyanobacteria, Firmicutes, Campilobacterota and Desulfobacterota, Proteobacteria (Alpha and Gamma divisions) (2–20 %; Fig. 4b). Gamma-Proteobacteria appeared to be the most abundant phylum in most time intervals and at most sites except for BNE. Cyanobacteria was more abundant in the dry season than in the wet season, and vice versa for Campilobacterota and Desulfobacterota (Fig.4b). For BNE, Bacteroidota constituted the major phylum for two out of three dry season samples. Firmicutes combined with Gamma-Proteobacteria outnumbered (>54%) the others during the wet season and January. Among all detected ASVs, ASVs with sequences related to Thiotrichaceae, Erysipelotrichaceae, and Phormidiaceae represented the most abundant ones. However, their abundances varied dramatically among sites.

Analyses of beta diversity revealed that microbial community compositions broadly clustered in accordance with time, regardless of sites (Fig. 5). Dry season samples were clustered (except BNE) and moderately separated from wet season samples. Wet season samples from the majority of sites (e.g., CWL01, DL, LY04, and MLL01) were scattered and showed a positive correlation with TSM, POC, and ^{13}C-POC. Notable exception was observed at site BNE, where samples deviated from the clustering pattern formed by the other sites and were correlated with elevated DOC levels.

https://doi.org/10.5194/egusphere-2025-5904
Preprint. Discussion started: 4 December 2025

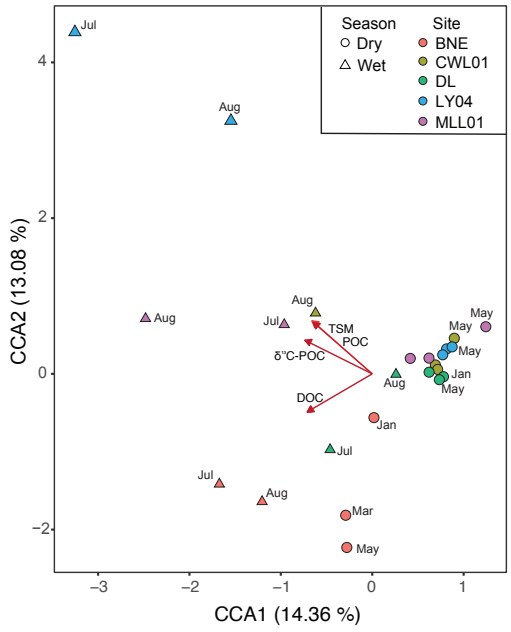

Figure 5. CCA ordination plot for beta diversity based on Bray-Curtis dissimilarity for 16S rRNA gene amplicons. Significant correlations (p <0.01) of geochemical parameters (solid lines with arrows) were projected as vectors onto the ordination.

4. Discussion

4.1 Solute and nutrient status, and river metabolism

The general physicochemical characteristics of river water (pH, major ions, TOC, TSM, and ^{13}C-DIC) were comparable with the data reported previously (Wang et al., 2024). These solute characteristics are mostly derived from carbonate dissolution (>80% of the total solute loads) driven by sulfuric acid produced by microbially mediated pyrite oxidation (Wang et al., 2024). Considering that a great portion of discharge is attributed to monsoon or typhoon, solute yields from carbonate dissolution during these extreme events dominate over the quiescent period and could be translated to a significant flux of CO_2 emission that constitutes a disproportionally large fraction of global flux (~1% from 0.002% of three major catchments in Taiwan). The high contribution pattern of carbonate weathering to the solute budget has also been observed for other active orogens (e.g., New Zealand and Himalayas) (Emberson et al., 2016; Kemeny et al., 2021). Furthermore, high water regime during summer monsoon or typhoons drains erodible materials (sediments accumulated in banks or hillslopes) into channels. As a result, TSM concentrations increased to a range of hundreds of mg L^{-1} by up to a factor of 40 (at LY04) between the wet and dry seasons (Table 2). This magnitude is far less than previous observations during the extreme events (up to 10 g L^{-1}; Dadson et al. 2003; Kao and Milliman 2008; Wang et al., 2024), given that the annual precipitation during the sampling period was much less than previous years (1858 mm for this study period versus ten-year average of 3402 mm for the most upstream Siangyang weather station; CWB annual report), but could still be sufficient to influence the expression of investigated metabolisms (see the next section). Similar increases in POC concentrations were also observed (Table 2). For comparison, inorganic solute concentrations exhibit various degrees of dilution caused by the increase in discharge.

https://doi.org/10.5194/egusphere-2025-5904
Preprint. Discussion started: 4 December 2025

While nitrate/nitrite and phosphate concentrations were rather invariable, Chl-a and ammonium concentrations were generally greater during the dry and wet seasons than the counterpart seasons, respectively (Table 2). As ammonium represents the degradative product of organic particulates, the higher ammonium concentrations in the wet season suggest either higher organic degradation along river transit or the purging of soil porewater more extensively during high water regime (Calmels et al., 2011). It is also worth noting that the comparable nitrate/nitrite and phosphate concentrations between seasons or higher ammonium concentrations in the wet season could be translated into a higher yield of these nutrients given a much higher discharge. As indicated by our results, organic degradation in river water did occur across all investigated sites distributed from the upstream to estuary. Their rates ranged from 0.3 to 12.9 μM hr^{-1}. Assuming a C/N ratio of ~5 for organic substrate (Lien et al., 2025), the total nitrogen rate produced from organic degradation would be 0.06 to 2.58 μM hr^{-1}. To reach the observed total dissolved inorganic nitrogen concentration (3.0 – 52.4 μM), net accumulation of nitrogen for 1.2–873 hours would be needed. Such a duration can be equivalent to a transport distance of at least 9 km for a velocity of 2.0 m s^{-1} during high water period. Given the overall river length is about 80 km, the residence time required to reach the observed nitrogen nutrient concentration is likely but challenging. Alternatively, soil development is limited in the investigated catchment. High erosion and heavy precipitation associated with extreme hydrologic events could have drained the stagnant soil porewater along with soil particulates and groundwater residing in fracture network rapidly into the rivers. As these water bodies preserve the degradative products of organic matters and their transport is slow (Alley et al., 2002; Calmels et al., 2011), these nutrient constituents would be accumulated to a high level during the quiescent period and only be rapidly purged when the erosion and high hydraulic head are imposed. High frequency monitoring of river water and groundwater across the event period is warranted to gauge the mechanism of nutrient release from the soil. Finally, such a data pattern is also comparable with nutrient deprived oligotrophic state commonly observed for open ocean (Overholt et al., 2022).

Furthermore, Chl-a concentrations were enhanced by a factor of at least 2.2 during the dry season when compared with the wet season (except for site DL). Pearson correlation analysis revealed a significant negative correlation between Chl-a and TSM ($r = –0.46$, $p < 0.05$) and no significant correlation between Chl-a and POC ($r = –0.41$, $p = 0.06$) (Table S4). Chl-a concentrations at sites MLL01 and LY04 during the wet season were barely detectable. While nutrient concentrations (nitrate/nitrite and phosphate) do not vary considerably between sites, nutrients do not appear to be a deterministic factor in controlling phototrophic activity. Instead, the load of suspended sediment can affect the expression of phototrophy even at a scale of hundreds of mg L^{-1}, a level that is not particularly unusual for mountainous rivers. Potential mechanisms inhibiting phototrophic activity include the shading created by dense sediments, grain pulverization, and abrasion (Stanley et al., 2010). The results are consistent with O'Donnell and Hotchkiss (2022), who found that the primary production and ecosystem respiration impacted by high flow events departed from the baseline represented by the mean daily metabolism based on continuous dissolved oxygen concentrations (O'Donnell and Hotchkiss, 2022). Their results also indicate that both GPP and ER rates were reduced by flash flow with GPP rates varying at a greater magnitude than ER (Blaszczak et al., 2019; Hall et al., 2015).

4.2 Autotrophic carbon fixation: rates and controlling factors

To further investigate the effect of environmental factors on metabolic rates, analyses of the Pearson correlation were performed (Fig. S3). DIC uptake rates were significantly influenced by TSM, POC, δ^{13}C-POC, and ammonium regardless of light availability. Under light conditions, DIC rates were also significantly correlated with temperature, DOC, and nutrients. An examination of detailed DIC rates for the wet season further revealed that rate variation could be divided into two categories. The first category is represented by sites CWL01, DL, and BNE where rates with light were higher

https://doi.org/10.5194/egusphere-2025-5904
Preprint. Discussion started: 4 December 2025

than those without light (Fig. 3a,b). The largest difference at 43 mg-C m^{-3} d^{-1} was recovered from the most downstream site BNE (Table S2). The second category is represented by sites MLL01 and LY04 where rates with light were either comparable with or slightly less than those without light. For incubations with DIC for the dry season, rates with light were generally much larger than those without light. In fact, rates without light were below the detection for sites MLL01, DL, and BNE. The only exception occurs for site CWL01 where DIC uptake rates with light were slightly higher than those without light. The results in part corroborate the Chl-a pattern but offer an additional dimension for constraining river metabolism. Differences in rates with and without light could be interpreted as the phototrophic rates assuming that lithoautotrophic rates (obtained from dark conditions) are constant regardless of whether light is available. In this regard, phototrophic rates for sites MLL01 and LY04 were lower in the wet season and even completely inhibited with the replacement of lithoautotrophy. In contrast, phototrophic rates were greater in the wet season than in the dry season for the other three sites even though lithoautotrophy was substantially reduced during the dry season. Additionally, the significantly positive correlations between DIC rates under light conditions and TSM, POC, and δ^{13}C-POC contradict with the expression of phototrophy. This pattern could be largely accounted for by the fact that a large fraction of the DIC rates with light (115-145%) were attributed to the lithoautotrophic rates during the wet season (Table S2). Therefore, the significant correlation for light conditions resembles that for dark conditions. By comparison, the significant correlation between the difference in DIC rate and nutrient concentration is compatible with the fact that the primary production is highly dependent on the nutrient availability in aquatic environments (Cloern, 1999; Domingues et al., 2005). As the nutrients generated from the degradation of organic matters accumulate along the river flow, BNE was characterized by the highest concentrations of nutrients and phototrophic rates in the wet season (Fig. 3). Notably, the Chl-a concentration didn't show a significant correlation to the phototrophic rate (the difference in DIC rate under light and dark conditions) (Fig. S3).

4.3 Particulate-mediated lithoautotrophy in the wet season

The incubation with DIC under dark conditions yielded DIC uptake rates spanning from lower than the detection to 1.6 mg-C m^{-3} h^{-1} (Fig. 3). These rates constitute mostly a small fraction (<5%) of the rates under light conditions but become generally high and even comparable with the rates under light conditions for samples collected during the period of high sediment load (LY04 and MLL01 in August). The rate pattern is intriguing and suggests the intimate relationships with the potential substrates supplied from the suspended particulates or reduced ions from the groundwater influx. For particulate matters, potential substrates include reduced sulfur or iron-bearing minerals (e.g., pyrite) and ammonium encapsulated within the interlayer of clay minerals (Petit et al., 2006). Pyrite is prevalently distributed in meta-sedimentary rocks of the catchment and has been identified as the main solute and CO_2 contributor of weathering (Blattmann et al., 2019; Bufe et al., 2021). A previous study conducted on the same catchment has shown a highly positive correlation of the yields between riverine sulfate, suspended sediment, and sulfur oxidizer (mainly composed of *Thiobacillus* and *Sulfuricurvulum* members) (Wang et al., 2024). The data pattern suggests that sulfate/sulfuric acid is primarily generated by the microbially mediated oxidation of pyrite in erodible materials in riparian zones or hillslopes. As the torrential precipitation proceeds, these materials along with the sulfur oxidizers are drained into the river channels and recovered by sampling and analysis. The data corroborate with the fact that erosion of bedrocks and the following pulverization on hillslopes or in river channels facilitate the exposure of pyrite to the atmosphere or air-infiltrated pore space, thereby rendering the oxidative reaction that produces sulfuric acid for dissolution of carbonate or other minerals (Hilton and West, 2020). Furthermore, the particulate pulverization and abrasion can also disrupt the cleavage or interlayer structure of clay minerals, thereby releasing ammonium into the surrounding (Yu et al., 2023). While river water is presumably saturated with the atmospheric oxygen, pyrite and ammonium associated with suspended particulates are readily available

https://doi.org/10.5194/egusphere-2025-5904
Preprint. Discussion started: 4 December 2025

for lithoautotrophic microbial exploitation and colonization. For groundwater influx for river, potential substrates for lithoautotrophy include ferrous iron, ammonium, and sulfide, all of which could be produced by either microbial reduction of oxidants (e.g., iron oxyhydroxide, nitrate, and sulfate) or organic degradation (for the release of ammonium). Considering that sulfate minerals have not been identified or recovered from the catchment to date, ferrous iron and ammonium produced in subsurface aquifers could be drained and discharged into rivers. Indeed, ammonium concentrations were significantly higher for the wet than for the dry seasons (Table 2). Our current analyses also revealed that potential sulfur oxidizers related to these two genera (*Thiobacillus* and *Sulfuricurvulum* members) and others (e.g., *Sulfurovum*, *Sulfurifustis*) and ammonium oxidizers related to *Nitrosomonas* and *Nitrosopumilus* constituted a significant proportion of communities (>10%) in the wet season as compared to 5% in the dry season. Detailed experiment design is required to pinpoint the exact substrate involved in the aquatic lithoautotrophy.

4.4 Heterotrophic amino acid metabolism and controlling factors

In contrast to autotrophic carbon fixation, heterotrophic metabolism showed distinct seasonal patterns and substrate preferences. Glycine and leucine uptake rates were correlated with nutrients and particulate characteristics (concentration and isotopic composition), respectively (Fig. S3). As the nutrients represent the degradative product of organic particulates, these relationships seem to suggest that the direct uptake of amino acids by riverine community members is linked to the metabolites generated by particulate degradation (for glycine) or particulate-associated populations (for leucine). For the former scenario, metabolites or nutrients released from the particulate degradation facilitate to boost the activity of a riverine population preferentially for glycine uptake. Such a relationship is analogous to the priming effect on soil microbiota where the addition of exogenous substrate or substance promotes further degradation of organic matters (Blagodatskaya and Kuzyakov 2008; Chen et al., 2014). On the other hand, the latter scenario suggests that the leucine uptake is intimately related to the size of the population attached to particulate organic matters. With a larger influx of TSM in the wet season, the size of the attached population could have been correspondingly enhanced, providing an amplified body of microorganisms with functional preferences on leucine uptake. The inference also suggests a divergent modulation of physiological preferences on glycine and leucine uptakes mediated by two distinct populations. The inference may be better constrained by expending the incubations to various concentrations of particulates and simultaneous analyses of stable isotope probing of cellular components (proteins, lipids, or nucleic acids) to identify the plausible populations actively incorporating either of these amino acids.

The exploitability of organic substrates for heterotrophy is worth noting. Glycine uptake rates were generally higher than leucine uptake rates for the wet season (except for LY04, where both rates were comparable) (Fig. 3c). In the dry season, these two uptake rates were comparable but noticeably much lower than those in the wet season. For comparison, glycine catabolic rates were higher than leucine catabolic rates for CWL01, DL, and LY04 in the wet season. Both rates were comparable to each other at other sites (Fig. 3d). Overall, the selectivity of glycine over leucine for the wet season was prevalent (at four out of five sites for uptake and three out of five sites for catabolism). The cause of substrate selectivity may be attributed to the preferential utilization of simply structured substrate by specific community members or enzymatic expression (Geisseler and Horwath 2014; Palenik and Morel 1990). As both amino acids are required for biosynthesis, more experiments are needed to clarify the expression of specific pathway.

The results for heterotrophic incubations in this study revealed that catabolic rates exceeded assimilation rates by at least two orders of magnitude (Fig. S4). Except for January incubation with leucine for CWL01, all the other incubations with amino acids yielded a ratio of catabolic to uptake rates for January greater than for August. The ratios even reached an infinite level (uptake rate below the detection) for MLL01 and DL in January. The overwhelmingly large ratios were

https://doi.org/10.5194/egusphere-2025-5904
Preprint. Discussion started: 4 December 2025

primarily controlled by heterotrophic assimilation at extremely low levels during the dry season when sediment supply was low. Although the incubations were provided with readily available amino acids, the slow assimilation suggests that the communities in the dry season were customized to a deprived supply of nutrients and small organic molecules generated from the degradation of particulate organic matter. Therefore, any solid or soluble substrate available for microbial utilization would be initially diverted to catabolism for energy generation to sustain certain maintenance activities (McInerney et al., 2010). Thus, even when the amino acids were provided during incubations, their assimilation was not immediately enhanced under such energy-limited conditions for heterotrophs. Conversely, communities in the wet season were accessible to the abundant supply of particulate organic matters to catalyze metabolisms for energy generation or assimilation. Consequently, a relative smaller fraction of the fed amino acids were diverted to assimilation or biosynthesis. Nevertheless, the heterotrophy in such oligotrophic mountainous rivers yields excessive CO_2 that is susceptible to the net emission through the air-water exchange.

4.5 Implications for river heterotrophy and carbon cycling

The rate comparison between autotrophy and heterotrophy (assimilation plus catabolism) indicates that the Beinan river is net heterotrophic, producing excess CO_2 through planktonic microbial processes. As the incubations were performed over a short period of time (4–6 hrs), the physiological status of community members may resemble the *in situ* conditions after this short period. In this regard, the derived rates were considered to bracket the range of true rates. It is worth noting that the current estimates only constrain the metabolisms and rates for planktonic communities. As the benthic and hyporheic zones are connected and interact with river water, their communities can also contribute to the cycling of organic carbon. Therefore, the current results represent a conservative estimate of river metabolism. Planktonic metabolic CO_2 production (~10^7 mol yr^{-1}) accounts for less than 5% of both river-atmosphere CO_2 exchange flux (~2.6 x 10^9 mol yr^{-1}) and CO_2 production from chemical weathering (2.8 x 10^9 mol yr^{-1}; Wang et al., 2024) and petrogenic carbon oxidation (1.7-2.9 x 10^9 mol yr^{-1}; Lien et al., 2025). This pattern indicates that net CO_2 emissions through the river-air interface are overwhelmingly driven by the weathering of minerals and petrogenic carbon, with planktonic river metabolism playing a minor role in total catchment CO_2 evasion. While these estimates represent water column processes only, the potential benthic and hyporheic contributions may have been reduced during the high-water period by higher sediment mobility and limited light penetration (Battin et al. 2023; Hall et al., 2015). The overall contribution of river metabolisms (sum of planktonic, benthic, and hyporheic metabolisms) would be unlikely to substantially alter the dominance of weathering-derived CO_2.

Previous studies based on dissolved oxygen data demonstrate that both fluxes of net ecosystem production (NEP) and CO_2 emissions derived from river-air exchange vary over several orders of magnitude as the discharge or stream order increases for the catchments distributed over contiguous US and European boreal regions (Dodds et al., 2013; Cory et al., 2014; Hotchkiss et al., 2015; Rasilo et al., 2017; Lupon et al., 2019; Bernal et al., 2022). Using a discharge-weighted regression, Hotchkiss et al. (2015) found that NEP fluxes varied much less. Such a regional data pattern also suggests that the contribution fraction of NEP to the total emission increases from ~15% to ~50% as the discharge increases to hundreds of cms (cubic meter per second). Only limited data simultaneously covering NEP, CO_2 emissions, and discharge are available for individual catchments. These studies show that the fractions range from 17% to 75% for rivers in Canada (Rasilo et al., 2017), from 17% to 51% in Sweden (Lupon et al., 2019), ~22% in southeastern US (Dodds et al., 2013), and from 51% to 57% in northeastern Spain (Bernal et al., 2022). Recent modeling for catchments in contiguous US suggests that the NEP accounts for ~7% of the total evasion (Maavara et al., 2025). The fractions (<5%) reported herein are even smaller than any fraction obtained in previous studies. Such a low range of NEP/exchange fluxes is in great

https://doi.org/10.5194/egusphere-2025-5904
Preprint. Discussion started: 4 December 2025

contrast to most of the examples obtained elsewhere, even for the site (BNE) located nearest to the shoreline or with the greatest stream order (SO = 5). The pattern suggests that steep topography and rapid erosion associated with active mountain building limite the development of soils, a scarce supply of nutrients, and rapid transit of river water, all of which apparently restrain the expression of river metabolisms. In contrast, voluminous amounts of metamorphic rocks are fractured and eroded, providing unlimited materials readily for the oxidation of pyrite and petrogenic carbon mediated by microbial processes in the subsurface and river banks (Wang et al., 2024; Lien et al., 2025). In consequence, CO_2 generated by these weathering reactions is drained into the river along with groundwater flow and dominates over the contribution from other sources.

4.6 Seasonal and spatial dynamics of microbial communities

Variations in community diversity and composition were evident across different sites and sampling periods. Beta analysis indicated that microbial community compositions generally varied over time across most sites (Fig 5). Samples collected during the dry season were clustered, with the exception of BNE, and moderately deviated from those collected during the wet season. Based on these ordination patterns and a detailed taxonomic analysis, the sites can be categorized into three distinct groups: those exhibiting clear seasonal patterns (MLL01, CWL01, LY04), site with complex temporal dynamics that do not strictly follow seasonal variation (DL), and the most downstream site (BNE) where communities for different months are scattered at a great extent.

MLL01 and LY04 exhibited the most pronounced seasonal trends in community diversity and composition (Figs. 4, 5). Community diversity was lower during the wet season than the dry season, except for the one in January at MLL01 (Fig. 4a). During the dry season, communities at both sites were predominantly composed of lithoautotrophs (Table S7). More specifically, MLL01 and LY04 were dominated by iron-oxidizing *Sideroxydans*, and sulfur-oxidizing *Thiothrix*, respectively. Both genera utilize the Calvin-Benson-Bassham cycle for carbon fixation (Emerson et al., 2010, 2013; Grabovich et al., 2023; Ravin et al., 2021). Major members in communities shifted towards different compositions in the wet season, such as autotrophic *Sulfuricurvum* and *Thiobacillus* (sulfur-oxidizing) at MLL01 and a combination of autotrophic and heterotrophic taxa at LY04 (*Thiobacillus*, *Arenimonas*, and Coxiellaceae). The presence of heterotrophic Coxiellaceae during the wet season coincided with increased TSM and POC levels, suggesting their introduction through terrestrial runoff rather than *in situ* growth and the impact of hydrological changes on community compositions. CWL01 was characterized by high community diversity during the sampling period except in January (Fig. 4a), and showed a distinct seasonal pattern in a way that lithoautotrophic genera (*Sulfuricurvum* and *Thiobacillus*) were more abundant in August, while Cyanobacteria dominated throughout the dry season (Fig 4b). This interpretation partially aligns with the low dark DIC uptake rates (Fig. 3). The patterns also suggest that abundances of lithoautotrophic and photosynthetic communities are complementary to each other in different seasons.

DL was characterized by an intricate temporal pattern that did not follow the distinct dry-wet seasonal variations, as described previously. Community diversity remained relatively stable across the seasons (Fig. 4). The communities during the dry season (January, March, and May) clustered more tightly than the others (Fig. 5) and were predominantly composed of Cyanobacteria and *Thiothrix,* along with various heterotrophs (e.g., Comamonadaceae and Microscillaceae). The community in August also resembled those in the dry season and was dominated by *Thiothrix* and *Nitrospira*, highlighting the importance of sulfur and nitrogen metabolisms. However, the community in July deviated from this cluster and was dominated by the heterotrophic *Bacillus*. Such temporal variability of community variation was also correlated with DOC, suggesting that the extent of organic degradation and hydrological circulation plays a role.

https://doi.org/10.5194/egusphere-2025-5904
Preprint. Discussion started: 4 December 2025

The most downstream site, BNE, was notably distinct from all other mountainous sites. It was characterized by relatively low community diversity throughout the sampling period (except for January) (Fig. 4) and high community variation between campaigns. (Fig. 5). The communities for March and May were dominated by *Fluviicola*, a genus specializing in degrading complex organic compounds (Woyke et al., 2011). For July and August, the community compositions shifted to the predominance of *Turicibacter* and *Polynucleobacter*, both of which are capable of decomposing dissolved organic matter (Bosshard et al., 2002; Watanabe et al., 2012). The prevalence of heterotrophic taxa throughout all seasons was consistent with a high glycine catabolic rate (Fig. 3) and a significant correlation between community variation and DOC concentration (Fig. 5). The pattern also reflects its downstream role, where organic matter accumulated along the drainage path facilitates heterotrophic respiration.

Overall, chemolithoautotrophs, such as *Sideroxydans*, *Thothrix*, *Sulfuricuvum*, and *Thiobacillus* were abundant during the wet season, whereas phototrophs and heterotrophs dominated during the dry season at the mountainous sites. For BNE, abundant heterotrophs (*Fluviicola, Turicibacter* and *Polynucleobacter*) were observed throughout the seasons even though the constituted genera were different. Such community pattern and inferred metabolism were not consistent with the rate measurements, suggesting the numerically abundant community members were not equivalently or proportionally metabolically expressed. Further studies on RNA are warranted to investigate the composition of active community members.

Conclusions

This study elucidates the dynamic nature of river metabolisms in the Beinan River system. By supplementing ^{13}C-labelled substrates, our incubations yielded that all categories of metabolic rates were consistently higher during the wet season than the dry season, and that heterotrophic rates were higher than autotrophic rates. The deduced net metabolic CO_2 rates at ~10^7 mol yr^{-1} account for less than 5% of the exchange of CO_2 at the air-water interface, pyrite-induced weathering, and petrogenic carbon oxidation. Microbial community compositions shifted from lithoautotrophs (sulfur and nitrogen metabolizers) in the wet season to a mixture of phototrophs and heterotrophs in the dry season, reflecting the dynamic response of biological processes to variations in hydrology and particle loading in the river. While planktonic metabolic rates are not as significant as those for major river systems, these findings highlight the complexity and dynamics of river metabolisms and microbial communities in tectonically active mountainous catchments prone to intense hydrological events and rapid landscape changes.

Author contribution

Jhen-Nien Chen: conceptualization; formal analysis; investigation; methodology; writing—original draft. Pei-En Chen: conceptualization; methodology; formal analysis; writing—original draft; Yu-Shiang Yen: methodology; formal analysis; investigation. Tzu-Hsuan Tu: conceptualization; methodology; writing - review & editing. Lu-Yu Wang: conceptualization; methodology; data curation. Wan-Yin Lien: conceptualization; formal analysis; writing - review & editing. Yueh-Ting Lin: conceptualization; data curation; writing - review & editing. Pei-Ling Wang: Conceptualization; funding acquisition; investigation; methodology; project administration; resources; supervision; validation; writing—review and editing.

Competing interests

The authors declare that they have no conflict of interest.

https://doi.org/10.5194/egusphere-2025-5904
Preprint. Discussion started: 4 December 2025

Acknowledgements

We are grateful for the funding support from the Taiwanese MOE and NSTC to THT (NSTC 113-2116-M-110-002) and PLW (NSTC 113-2116-M-002-027, MOE 113L901005). We also acknowledge the logistical support and comments provided by Li-Hung Lin and the assistance in sampling and geochemical analyses by Ya-Fang Cheng, Tzu-Jung Cheng, Yun-Hsuan Lee, Ruei-Feng Tsai, Bo-Yu Chen, Jing-Yi Tseng, and Ling-Wen Liu.

References

Alfreider, A., Vogt, C., Hoffmann, D., and Babel, W.: Diversity of Ribulose-1,5-Bisphosphate Carboxylase/Oxygenase Large-Subunit Genes from Groundwater and Aquifer Microorganisms, Microb. Ecol., 45, 317–328, https://doi.org/10.1007/s00248-003-2004-9, 2003.

Allen, G. H. and Pavelsky, T. M.: Global extent of rivers and streams, Science, 361, 585–588, https://doi.org/10.1126/science.aat0636, 2018.

Alley, W. M., Healy, R. W., LaBaugh, J. W., and Reilly, T. E.: Flow and Storage in Groundwater Systems, Science, 296, 1985–1990, https://doi.org/10.1126/science.1067123, 2002.

Appling, A. P., Hall, R. O., Yackulic, C. B., and Arroita, M.: Overcoming Equifinality: Leveraging Long Time Series for Stream Metabolism Estimation, J. Geophys. Res. Biogeosciences, 123, 624–645, https://doi.org/10.1002/2017JG004140, 2018.

Aufdenkampe, A. K., Mayorga, E., Raymond, P. A., Melack, J. M., Doney, S. C., Alin, S. R., Aalto, R. E., and Yoo, K.: Riverine coupling of biogeochemical cycles between land, oceans, and atmosphere, Front. Ecol. Environ., 9, 53–60, https://doi.org/10.1890/100014, 2011.

Bandyopadhyay, J., Kraemer, D., Kattelmann, R. and Kundzewicz, Z. W.: Highland waters: A resource of global significance, in Mountains of the World: A Global Priority, edited by B. Messerli and J. Ives, pp. 131 – 155, Parthenon, New York. 1997.

Battin, T. J., Lauerwald, R., Bernhardt, E. S., Bertuzzo, E., Gener, L. G., Hall, R. O., Hotchkiss, E. R., Maavara, T., Pavelsky, T. M., Ran, L., Raymond, P., Rosentreter, J. A., and Regnier, P.: River ecosystem metabolism and carbon biogeochemistry in a changing world, Nature, 613, 449–459, https://doi.org/10.1038/s41586-022-05500-8, 2023.

Bernal, S., Cohen, M. J., Ledesma, J. L. J., Kirk, L., Martí, E., and Lupon, A.: Stream metabolism sources a large fraction of carbon dioxide to the atmosphere in two hydrologically contrasting headwater streams, Limnol. Oceanogr., 67, 2621–2634, https://doi.org/10.1002/lno.12226, 2022.

Blagodatskaya, E. and Kuzyakov, Y.: Mechanisms of real and apparent priming effects and their dependence on soil microbial biomass and community structure: critical review, Biol. Fertil. Soils, 45, 115–131, https://doi.org/10.1007/s00374-008-0334-y, 2008.

Blaszczak, J. R., Delesantro, J. M., Urban, D. L., Doyle, M. W., and Bernhardt, E. S.: Scoured or suffocated: Urban stream ecosystems oscillate between hydrologic and dissolved oxygen extremes, Limnol. Oceanogr., 64, 877–894, https://doi.org/10.1002/lno.11081, 2019.

Blattmann, T. M., Wang, S.-L., Lupker, M., Märki, L., Haghipour, N., Wacker, L., Chung, L.-H., Bernasconi, S. M., Plötze, M., and Eglinton, T. I.: Sulphuric acid-mediated weathering on Taiwan buffers geological atmospheric carbon sinks, Sci. Rep., 9, 2945, https://doi.org/10.1038/s41598-019-39272-5, 2019.

Bolyen, E., Rideout, J. R., Dillon, M. R., Bokulich, N. A., Abnet, C. C., Al-Ghalith, G. A., Alexander, H., Alm, E. J., Arumugam, M., Asnicar, F., Bai, Y., Bisanz, J. E., Bittinger, K., Brejnrod, A., Brislawn, C. J., Brown, C. T., Callahan, B. J., Caraballo-Rodríguez, A. M., Chase, J., Cope, E. K., Da Silva, R., Diener, C., Dorrestein, P. C., Douglas, G. M., Durall, D. M., Duvallet, C., Edwardson, C. F., Ernst, M., Estaki, M., Fouquier, J., Gauglitz, J. M., Gibbons, S. M.,

https://doi.org/10.5194/egusphere-2025-5904
Preprint. Discussion started: 4 December 2025

Gibson, D. L., Gonzalez, A., Gorlick, K., Guo, J., Hillmann, B., Holmes, S., Holste, H., Huttenhower, C., Huttley, G. A., Janssen, S., Jarmusch, A. K., Jiang, L., Kaehler, B. D., Kang, K. B., Keefe, C. R., Keim, P., Kelley, S. T., Knights, D., Koester, I., Kosciolek, T., Kreps, J., Langille, M. G. I., Lee, J., Ley, R., Liu, Y.-X., Loftfield, E., Lozupone, C., Maher, M., Marotz, C., Martin, B. D., McDonald, D., McIver, L. J., Melnik, A. V., Metcalf, J. L., Morgan, S. C., Morton, J. T., Naimey, A. T., Navas-Molina, J. A., Nothias, L. F., Orchanian, S. B., Pearson, T., Peoples, S. L., Petras, D., Preuss, M. L., Pruesse, E., Rasmussen, L. B., Rivers, A., Robeson, M. S., Rosenthal, P., Segata, N., Shaffer, M., Shiffer, A., Sinha, R., Song, S. J., Spear, J. R., Swafford, A. D., Thompson, L. R., Torres, P. J., Trinh, P., Tripathi, A., Turnbaugh, P. J., Ul-Hasan, S., Van Der Hooft, J. J. J., Vargas, F., Vázquez-Baeza, Y., Vogtmann, E., Von Hippel, M., et al.: Reproducible, interactive, scalable and extensible microbiome data

Bosshard, P. P., Zbinden, R., and Altwegg, M.: Turicibacter sanguinis gen. nov., sp. nov., a novel anaerobic, Gram-positive bacterium., Int. J. Syst. Evol. Microbiol., 52, 1263–1266, https://doi.org/10.1099/00207713-52-4-1263, 2002.

Brunke, M. and Gonser, T.: The ecological significance of exchange processes between rivers and groundwater, Freshw. Biol., 37, 1–33, https://doi.org/10.1046/j.1365-2427.1997.00143.x, 1997.

Bufe, A., Hovius, N., Emberson, R., Rugenstein, J. K. C., Galy, A., Hassenruck-Gudipati, H. J., and Chang, J.-M.: Co-variation of silicate, carbonate and sulfide weathering drives CO2 release with erosion, Nat. Geosci., 14, 211–216, https://doi.org/10.1038/s41561-021-00714-3, 2021.

Butman, D. and Raymond, P. A.: Significant efflux of carbon dioxide from streams and rivers in the United States, Nat. Geosci., 4, 839–842, https://doi.org/10.1038/ngeo1294, 2011.

Calmels, D., Galy, A., Hovius, N., Bickle, M., West, A. J., Chen, M.-C., and Chapman, H.: Contribution of deep groundwater to the weathering budget in a rapidly eroding mountain belt, Taiwan, Earth Planet. Sci. Lett., 303, 48–58, https://doi.org/10.1016/j.epsl.2010.12.032, 2011.

Chao, A.: Estimating the Population Size for Capture-Recapture Data with Unequal Catchability, Biometrics, 43, 783–791, https://doi.org/10.2307/2531532, 1987.

Chen, R., Senbayram, M., Blagodatsky, S., Myachina, O., Dittert, K., Lin, X., Blagodatskaya, E., and Kuzyakov, Y.: Soil C and N availability determine the priming effect: microbial N mining and stoichiometric decomposition theories, Glob. Change Biol., 20, 2356–2367, https://doi.org/10.1111/gcb.12475, 2014.

Chen, W.-S., Yeh, J.-J., and Syu, S.-J.: Late Cenozoic exhumation and erosion of the Taiwan orogenic belt: New insights from petrographic analysis of foreland basin sediments and thermochronological dating on the metamorphic orogenic wedge, Tectonophysics, 750, 56–69, https://doi.org/10.1016/j.tecto.2018.09.003, 2019.

Chiriboga, G. and Borges, A. V.: Andean headwater and piedmont streams are hot spots of carbon dioxide and methane emissions in the Amazon basin, Commun. Earth Environ., 4, 76, https://doi.org/10.1038/s43247-023-00745-1, 2023.

Cloern, J. E.: The relative importance of light and nutrient limitation of phytoplankton growth: a simple index of coastal ecosystem sensitivity to nutrient enrichment, Aquat. Ecol., 33, 3–16, 1999.

Cole, J. J., Prairie, Y. T., Caraco, N. F., McDowell, W. H., Tranvik, L. J., Striegl, R. G., Duarte, C. M., Kortelainen, P., Downing, J. A., Middelburg, J. J., and Melack, J.: Plumbing the Global Carbon Cycle: Integrating Inland Waters into the Terrestrial Carbon Budget, Ecosystems, 10, 172–185, https://doi.org/10.1007/s10021-006-9013-8, 2007.

Cory, R. M., Ward, C. P., Crump, B. C., and Kling, G. W.: Sunlight controls water column processing of carbon in arctic fresh waters, Science, 345, 925–928, https://doi.org/10.1126/science.1253119, 2014.

Dadson, S. J., Hovius, N., Chen, H., Dade, W. B., Hsieh, M.-L., Willett, S. D., Hu, J.-C., Horng, M.-J., Chen, M.-C., Stark, C. P., Lague, D., and Lin, J.-C.: Links between erosion, runoff variability and seismicity in the Taiwan orogen, Nature, 426, 648–651, https://doi.org/10.1038/nature02150, 2003.

https://doi.org/10.5194/egusphere-2025-5904
Preprint. Discussion started: 4 December 2025

669 Dodds, W. K., Veach, A. M., Ruffing, C. M., Larson, D. M., Fischer, J. L., and Costigan, K. H.: Abiotic controls and
670 temporal variability of river metabolism: multiyear analyses of Mississippi and Chattahoochee River data, Freshw. Sci.,
671 32, 1073–1087, https://doi.org/10.1899/13-018.1, 2013.

672 Domingues, R. B., Barbosa, A., and Galvão, H.: Nutrients, light and phytoplankton succession in a temperate estuary
673 (the Guadiana, south-western Iberia), Estuar. Coast. Shelf Sci., 64, 249–260, https://doi.org/10.1016/j.ecss.2005.02.017,
674 2005.

675 Duvert, C., Butman, D. E., Marx, A., Ribolzi, O., and Hutley, L. B.: CO2 evasion along streams driven by groundwater
676 inputs and geomorphic controls, Nat. Geosci., 11, 813–818, https://doi.org/10.1038/s41561-018-0245-y, 2018.

677 Emberson, R., Hovius, N., Galy, A., and Marc, O.: Chemical weathering in active mountain belts controlled by
678 stochastic bedrock landsliding, Nat. Geosci., 9, 42–45, https://doi.org/10.1038/ngeo2600, 2016.

679 Emerson, D., Fleming, E. J., and McBeth, J. M.: Iron-Oxidizing Bacteria: An Environmental and Genomic Perspective,
680 Annu. Rev. Microbiol., 64, 561–583, https://doi.org/10.1146/annurev.micro.112408.134208, 2010.

681 Emerson, D., Field, E. K., Chertkov, O., Davenport, K. W., Goodwin, L., Munk, C., Nolan, M., and Woyke, T.:
682 Comparative genomics of freshwater Fe-oxidizing bacteria: implications for physiology, ecology, and systematics,
683 Front. Microbiol., 4, https://doi.org/10.3389/fmicb.2013.00254, 2013.

684 Geisseler, D. and Horwath, W. R.: Investigating amino acid utilization by soil microorganisms using compound specific
685 stable isotope analysis, Soil Biol. Biochem., 74, 100–105, https://doi.org/10.1016/j.soilbio.2014.02.024, 2014.

686 González, I., Déjean, S., Martin, P., and Baccini, A.: **CCA** : An *R* Package to Extend Canonical Correlation Analysis, J.
687 Stat. Softw., 23, https://doi.org/10.18637/jss.v023.i12, 2008.

688 Grabovich, M. Yu., Ravin, N. V., and Boden, R.: *Thiothrix*, in: Bergey's Manual of Systematics of Archaea and
689 Bacteria, edited by: Whitman, W. B., Wiley, 1–21, https://doi.org/10.1002/9781118960608.gbm01229.pub2, 2023.

690 Hall, R. O., Yackulic, C. B., Kennedy, T. A., Yard, M. D., Rosi-Marshall, E. J., Voichick, N., and Behn, K. E.:
691 Turbidity, light, temperature, and hydropeaking control primary productivity in the Colorado River, Grand Canyon:
692 Semimechanistic modeling of daily GPP, Limnol. Oceanogr., 60, 512–526, https://doi.org/10.1002/lno.10031, 2015.

693 Hilton, R. G. and West, A. J.: Mountains, erosion and the carbon cycle, Nat. Rev. Earth Environ., 1, 284–299,
694 https://doi.org/10.1038/s43017-020-0058-6, 2020.

695 Hilton, R. G., Galy, A., Hovius, N., Chen, M.-C., Horng, M.-J., and Chen, H.: Tropical-cyclone-driven erosion of the
696 terrestrial biosphere from mountains, Nat. Geosci., 1, 759–762, https://doi.org/10.1038/ngeo333, 2008.

697 Horgby, Å., Segatto, P. L., Bertuzzo, E., Lauerwald, R., Lehner, B., Ulseth, A. J., Vennemann, T. W., and Battin, T. J.:
698 Unexpected large evasion fluxes of carbon dioxide from turbulent streams draining the world's mountains, Nat.
699 Commun., 10, 4888, https://doi.org/10.1038/s41467-019-12905-z, 2019.

700 Hotchkiss, E. R., Hall Jr, R. O., Sponseller, R. A., Butman, D., Klaminder, J., Laudon, H., Rosvall, M., and Karlsson, J.:
701 Sources of and processes controlling CO2 emissions change with the size of streams and rivers, Nat. Geosci., 8, 696–
702 699, https://doi.org/10.1038/ngeo2507, 2015.

703 Ives, J.D., Messerli, B. and Spiess, E., Introduction. In: Mountains of the World: A Global Priority, B. Messerli and J.D.
704 Ives (Eds.), Parthenon, New York and London, 115, 1997.

705 Jähne, B., Heinz, G., and Dietrich, W.: Measurement of the diffusion coefficients of sparingly soluble gases in water, J.
706 Geophys. Res. Oceans, 92, 10767–10776, https://doi.org/10.1029/JC092iC10p10767, 1987.

707 Kao, S. J. and Milliman, J. D.: Water and Sediment Discharge from Small Mountainous Rivers, Taiwan: The Roles of
708 Lithology, Episodic Events, and Human Activities, J. Geol., 116, 431–448, https://doi.org/10.1086/590921, 2008.

https://doi.org/10.5194/egusphere-2025-5904
Preprint. Discussion started: 4 December 2025

Kemeny, P. C., Lopez, G. I., Dalleska, N. F., Torres, M., Burke, A., Bhatt, M. P., West, A. J., Hartmann, J., and Adkins, J. F.: Sulfate sulfur isotopes and major ion chemistry reveal that pyrite oxidation counteracts CO2 drawdown from silicate weathering in the Langtang-Trisuli-Narayani River system, Nepal Himalaya, Geochim. Cosmochim. Acta, 294, 43–69, https://doi.org/10.1016/j.gca.2020.11.009, 2021.

Kozich, J. J., Westcott, S. L., Baxter, N. T., Highlander, S. K., and Schloss, P. D.: Development of a Dual-Index Sequencing Strategy and Curation Pipeline for Analyzing Amplicon Sequence Data on the MiSeq Illumina Sequencing Platform, Appl. Environ. Microbiol., 79, 5112–5120, https://doi.org/10.1128/AEM.01043-13, 2013.

Lauerwald, R., Laruelle, G. G., Hartmann, J., Ciais, P., and Regnier, P. A. G.: Spatial patterns in CO_2 evasion from the global river network, Glob. Biogeochem. Cycles, 29, 534–554, https://doi.org/10.1002/2014GB004941, 2015.

Lewis, E., and Wallace, D.: Program developed for CO2 system calculations. Ornl/Cdiac-105 1–21, 1998.

Lien, W.-Y., Chen, C.-T., Lee, Y.-H., Su, C.-C., Wang, P.-L., and Lin, L.-H.: Two-stage oxidation of petrogenic organic carbon in a rapidly exhuming small mountainous catchment, Commun. Earth Environ., 6, 45, https://doi.org/10.1038/s43247-025-02015-8, 2025.

Lin, B., Liu, Z., Eglinton, T. I., Kandasamy, S., Blattmann, T. M., Haghipour, N., Huang, K.-F., and You, C.-F.: Island-wide variation in provenance of riverine sedimentary organic carbon: A case study from Taiwan, Earth Planet. Sci. Lett., 539, 116238, https://doi.org/10.1016/j.epsl.2020.116238, 2020.

Lupon, A., Denfeld, B. A., Laudon, H., Leach, J., Karlsson, J., and Sponseller, R. A.: Groundwater inflows control patterns and sources of greenhouse gas emissions from streams, Limnol. Oceanogr., 64, 1545–1557, https://doi.org/10.1002/lno.11134, 2019.

Maavara, T., Yuan, Z., Johnson, A. M., Zhang, S., Aho, K. S., Brinkerhoff, C. B., Logozzo, L. A., and Raymond, P.: River metabolism in the contiguous United States: A West of extremes, Science, 390, 622–627, 2025.

Marx, A., Dusek, J., Jankovec, J., Sanda, M., Vogel, T., Van Geldern, R., Hartmann, J., and Barth, J. A. C.: A review of CO_2 and associated carbon dynamics in headwater streams: A global perspective, Rev. Geophys., 55, 560–585, https://doi.org/10.1002/2016RG000547, 2017.

McInerney, M. J., Hoehler, T., Gunsalus, R. P., and Schink, B.: Introduction to Microbial Hydrocarbon Production: Bioenergetics, in: Handbook of Hydrocarbon and Lipid Microbiology, edited by: Timmis, K. N., Springer Berlin Heidelberg, Berlin, Heidelberg, 319–335, https://doi.org/10.1007/978-3-540-77587-4_21, 2010.

McMillan, H. K. and Srinivasan, M. S.: Characteristics and controls of variability in soil moisture and groundwater in a headwater catchment, Hydrol. Earth Syst. Sci., 19, 1767–1786, https://doi.org/10.5194/hess-19-1767-2015, 2015.

Meybeck, M., Green, P., and Vörösmarty, C.: A New Typology for Mountains and Other Relief Classes: An Application to Global Continental Water Resources and Population Distribution, Mt. Res. Dev., 21, 34–45, https://doi.org/10.1659/0276-4741(2001)021%255B0034:ANTFMA%255D2.0.CO;2, 2001.

Miles, A. M., Chen, Y., Owens, M. W. and Grisham, M. B.: Fluorometric determination of nitric oxide. Methods A Companion to Methods Enzymol. 7: 40–47. doi:10.1006/meth.1995.1006, 1995.

O'Donnell, B. and Hotchkiss, E. R.: Resistance and resilience of stream metabolism to high flow disturbances, Biogeosciences, 19, 1111–1134, https://doi.org/10.5194/bg-19-1111-2022, 2022.

Overholt, W. A., Trumbore, S., Xu, X., Bornemann, T. L. V., Probst, A. J., Krüger, M., Herrmann, M., Thamdrup, B., Bristow, L. A., Taubert, M., Schwab, V. F., Hölzer, M., Marz, M., and Küsel, K.: Carbon fixation rates in groundwater similar to those in oligotrophic marine systems, Nat. Geosci., 15, 561–567, https://doi.org/10.1038/s41561-022-00968-5, 2022.

https://doi.org/10.5194/egusphere-2025-5904
Preprint. Discussion started: 4 December 2025

749 Palenik, B. and Morel, F.: Comparison of cell-surface L-amino acid oxidases from several marine phytoplankton, Mar.
750 Ecol. Prog. Ser., 59, 195–201, https://doi.org/10.3354/meps059195, 1990.

751 Petit, S., Righi, D. and Madejová, J.:Infrared spectroscopy of NH4+-bearing and saturated clay minerals: A review of
752 the study of layer charge. Appl. Clay Sci. **34**: 22–30. doi:10.1016/j.clay.2006.02.007, 2006

753 Quast, C., Pruesse, E., Yilmaz, P., Gerken, J., Schweer, T., Yarza, P., Peplies, J., and Glöckner, F. O.: The SILVA
754 ribosomal RNA gene database project: improved data processing and web-based tools, Nucleic Acids Res., 41, D590–
755 D596, https://doi.org/10.1093/nar/gks1219, 2012.

756 Rasilo, T., Hutchins, R. H. S., Ruiz-González, C., and Del Giorgio, P. A.: Transport and transformation of soil-derived
757 CO2, CH4 and DOC sustain CO2 supersaturation in small boreal streams, Sci. Total Environ., 579, 902–912,
758 https://doi.org/10.1016/j.scitotenv.2016.10.187, 2017.

759 Ravin, N. V., Rudenko, T. S., Smolyakov, D. D., Beletsky, A. V., Rakitin, A. L., Markov, N. D., Fomenkov, A., Sun,
760 L., Roberts, R. J., Novikov, A. A., Karnachuk, O. V., and Grabovich, M. Y.: Comparative Genome Analysis of the
761 Genus Thiothrix Involving Three Novel Species, Thiothrix subterranea sp. nov. Ku-5, Thiothrix litoralis sp. nov. AS
762 and "Candidatus Thiothrix anitrata" sp. nov. A52, Revealed the Conservation of the Pathways of Dissimilatory Sulfur
763 Metabolism and Variations in the Genetic Inventory for Nitrogen Metabolism and Autotrophic Carbon Fixation, Front.
764 Microbiol., 12, 760289, https://doi.org/10.3389/fmicb.2021.760289, 2021.

765 Raymond, P. A., Hartmann, J., Lauerwald, R., Sobek, S., McDonald, C., Hoover, M., Butman, D., Striegl, R., Mayorga,
766 E., Humborg, C., Kortelainen, P., Dürr, H., Meybeck, M., Ciais, P., and Guth, P.: Global carbon dioxide emissions from
767 inland waters, Nature, 503, 355–359, https://doi.org/10.1038/nature12760, 2013.

768 Saccardi, B. and Winnick, M.: Improving Predictions of Stream CO_2 Concentrations and Fluxes Using a Stream
769 Network Model: A Case Study in the East River Watershed, CO, USA, Glob. Biogeochem. Cycles, 35,
770 e2021GB006972, https://doi.org/10.1029/2021GB006972, 2021.

771 Schelker, J., Singer, G. A., Ulseth, A. J., Hengsberger, S., and Battin, T. J.: CO_2 evasion from a steep, high gradient
772 stream network: importance of seasonal and diurnal variation in aquatic pCO_2 and gas transfer: CO_2 evasion from a
773 steep, high gradient stream network, Limnol. Oceanogr., 61, 1826–1838, https://doi.org/10.1002/lno.10339, 2016.

774 Schloss, P. D., Westcott, S. L., Ryabin, T., Hall, J. R., Hartmann, M., Hollister, E. B., Lesniewski, R. A., Oakley, B. B.,
775 Parks, D. H., Robinson, C. J., Sahl, J. W., Stres, B., Thallinger, G. G., Van Horn, D. J., and Weber, C. F.: Introducing
776 mothur: Open-Source, Platform-Independent, Community-Supported Software for Describing and Comparing
777 Microbial Communities, Appl. Environ. Microbiol., 75, 7537–7541, https://doi.org/10.1128/AEM.01541-09, 2009.

778 Shannon, C. E., and Weaver, W.: The mathematical theory of communication., University of Illinois Press, 1949.

779 Stanley, E. H., Powers, S. M., and Lottig, N. R.: The evolving legacy of disturbance in stream ecology: concepts,
780 contributions, and coming challenges, J. North Am. Benthol. Soc., 29, 67–83, https://doi.org/10.1899/08-027.1, 2010.

781 Stanley R.S., Hill L.B., Chang H.C., and Hu H.N.: A transect through the metamorphic core of the Central Mountains,
782 southern Taiwan, in: Memoir of the Geological Society of China (Taiwan), vol. 4, 443–473, 1981.

783 Takahashi, T., Sutherland, S. C., Wanninkhof, R., Sweeney, C., Feely, R. A., Chipman, D. W., Hales, B., Friederich, G.,
784 Chavez, F., Sabine, C., Watson, A., Bakker, D. C. E., Schuster, U., Metzl, N., Yoshikawa-Inoue, H., Ishii, M.,
785 Midorikawa, T., Nojiri, Y., Körtzinger, A., Steinhoff, T., Hoppema, M., Olafsson, J., Arnarson, T. S., Tilbrook, B.,
786 Johannessen, T., Olsen, A., Bellerby, R., Wong, C. S., Delille, B., Bates, N. R., and De Baar, H. J. W.: Climatological
787 mean and decadal change in surface ocean pCO2, and net sea–air CO2 flux over the global oceans, Deep Sea Res. Part
788 II Top. Stud. Oceanogr., 56, 554–577, https://doi.org/10.1016/j.dsr2.2008.12.009, 2009.

789 Teng, L. S.: Geotectonic evolution of late Cenozoic arc-continent collision in Taiwan, Tectonophysics, 183, 57–76,
790 https://doi.org/10.1016/0040-1951(90)90188-E, 1990.

https://doi.org/10.5194/egusphere-2025-5904
Preprint. Discussion started: 4 December 2025

Tu, T.-H., Wu, L.-W., Lin, Y.-S., Imachi, H., Lin, L.-H., and Wang, P.-L.: Microbial Community Composition and Functional Capacity in a Terrestrial Ferruginous, Sulfate-Depleted Mud Volcano, Front. Microbiol., 8, 2137, https://doi.org/10.3389/fmicb.2017.02137, 2017.

Tu, T.-H., Chen, L.-L., Chiu, Y.-P., Lin, L.-H., Wu, L.-W., Italiano, F., Shyu, J. B. H., Raisossadat, S. N., and Wang, P.-L.: The biogeographic pattern of microbial communities inhabiting terrestrial mud volcanoes across the Eurasian continent, Biogeosciences, 19, 831–843, https://doi.org/10.5194/bg-19-831-2022, 2022.

Ulseth, A. J., Hall, R. O., Boix Canadell, M., Madinger, H. L., Niayifar, A., and Battin, T. J.: Distinct air–water gas exchange regimes in low- and high-energy streams, Nat. Geosci., 12, 259–263, https://doi.org/10.1038/s41561-019-0324-8, 2019.

Viviroli, D. and Weingartner, R.: The hydrological significance of mountains: from regional to global scale, Hydrol. Earth Syst. Sci., 8, 1017–1030, https://doi.org/10.5194/hess-8-1017-2004, 2004.

Wang, P.-L., Tu, T.-H., Lin, L.-H., Chou, H.-L., Wang, Y.-J., Chen, J.-N., Wang, L.-Y., Chang, J.-M., Chu, M.-F., Hsu, Y.-C., Chang, C.-P., Wu, Y.-M., Lin, Y.-T., and Ke, C.-C.: Microbial communities modulate chemical weathering and carbon dioxide cycling in an active orogen in Taiwan, Commun. Earth Environ., 5, 174, https://doi.org/10.1038/s43247-024-01345-3, 2024.

Wang, Y., Tian, R. M., Gao, Z. M., Bougouffa, S., and Qian, P. Y.: Optimal eukaryotic 18S and universal 16S/18S ribosomal RNA primers and their application in a study of symbiosis, PLoS ONE, 9, https://doi.org/10.1371/journal.pone.0090053, 2014.

Wanninkhof, R.: Relationship between wind speed and gas exchange over the ocean revisited, Limnol. Oceanogr. Methods, 12, 351–362, https://doi.org/10.4319/lom.2014.12.351, 2014.

Watanabe, K., Komatsu, N., Kitamura, T., Ishii, Y., Park, H., Miyata, R., Noda, N., Sekiguchi, Y., Satou, T., Watanabe, M., Yamamura, S., Imai, A., and Hayashi, S.: Ecological niche separation in the *Polynucleobacter* subclusters linked to quality of dissolved organic matter: a demonstration using a high sensitivity cultivation-based approach, Environ. Microbiol., 14, 2511–2525, https://doi.org/10.1111/j.1462-2920.2012.02815.x, 2012.

Woyke, T., Chertkov, O., Lapidus, A., Nolan, M., Lucas, S., Del Rio, T. G., Tice, H., Cheng, J.-F., Tapia, R., Han, C., Goodwin, L., Pitluck, S., Liolios, K., Pagani, I., Ivanova, N., Huntemann, M., Mavromatis, K., Mikhailova, N., Pati, A., Chen, A., Palaniappan, K., Land, M., Hauser, L., Brambilla, E.-M., Rohde, M., Mwirichia, R., Sikorski, J., Tindall, B. J., Göker, M., Bristow, J., Eisen, J. A., Markowitz, V., Hugenholtz, P., Klenk, H.-P., and Kyrpides, N. C.: Complete genome sequence of the gliding freshwater bacterium Fluviicola taffensis type strain (RW262T), Stand. Genomic Sci., 5, 21–29, https://doi.org/10.4056/sigs.2124912, 2011.

Yu, A. J., Lin, X., Zhu, J., He, H., and Li, L.: Environmental effects on ammonium adsorption onto clay minerals: Experimental constraints and applications, Appl. Clay Sci., 246, 107165, https://doi.org/10.1016/j.clay.2023.107165, 2023.